MATERIALS CHEMISTRY
FRONTIERS

RESEARCH ARTICLE

View Article Online
View Journal | View Issue

Cite this: *Mater. Chem. Front.*, 2025, **9**, 3057

What determines the iodine oxidation reaction kinetics in halide perovskite solar cells?

Rui Yang,† Xinyi Liu,† Yan Zhu, Qing Li, Peng Wang, Yangyue Zhang, Haotian Wu, Yu Peng, Shuang Yang * and Yu Hou *

Received 1st July 2025,
Accepted 25th August 2025

DOI: 10.1039/d5qm00466g

rsc.li/frontiers-materials

Perovskite solar cells (PSCs) have garnered significant attention owing to their solution fabrication, cost-effectiveness, and high power conversion efficiency, yet their practical application has been hindered by instability issues. Under operational conditions, redox reactions have been found to be prevalent in perovskite devices, but the underlying mechanism remains very unclear. Here, we systematically investigated the impact of light irradiation, atmosphere and interfacial structures on the redox kinetics in PSCs. Our results show that oxygen acts as a predominant factor driving device degradation, other than the transport layer or spectral components. Spectroscopic results reveal that the formation of iodine-related defects, *e.g.*, triiodide ion (I_3^-) and iodine (I_2), are dramatically boosted under oxygen-rich conditions, and can be further accelerated by light exposure. These findings provide critical insights into the redox reaction mechanism of perovskite-based materials, and offer a potential direction for enhancing the long-term stability of PSCs.

Introduction

PSCs have attracted considerable interest in the photovoltaics research community due to their high efficiency, low production cost, and exceptional optoelectronic properties.[1–6] Recently, PSCs have achieved a certified efficiency of 26.95%,[7] which is comparable to that of the silicon-based photovoltaics. However, numerous factors contribute to the instability of PSCs, ultimately leading to significant deterioration in their performance.[8–10]

Perovskites have been shown to be intrinsically unstable, as manifested by phase instability, low formation energy, and ion migration.[11–13] The constituents of perovskites, like iodide (I^-) and lead(II) ions (Pb^{2+}), often undergo redox reactions under operation. External factors, such as light exposure, temperature, humidity, oxygen, tensile stress, and electrical bias, have been substantiated to accelerate these redox-related degradation processes in perovskite-based devices.[14–18] For example, a hydration process disrupts the three-dimensional perovskite structure, leading to its decomposition into lead iodide (PbI_2) and hydroiodic acid (HI). These degradation products then undergo photoactivated redox reactions with atmospheric oxygen, ultimately producing metallic lead (Pb^0) and iodine (I_2) vapor through a series of photochemical oxidation processes.[19–21] Oxygen-induced reversible degradation has also been identified as a unique phenomenon in some PSCs. B. Purev-Ochir *et al.* found that exposure to oxygen can initially degrade the perovskite material, yet the reaction is reversible under certain conditions, such as in a vacuum environment.[22] When interfaced with metal oxides (such as titanium dioxide, TiO_2), it may trap charge carriers, and facilitate the generation of reactive oxygen species under illumination, which accelerates the photochemical degradation of perovskite materials.[23] First-principles calculation and spectroscopic analysis by Ambrosio *et al.* revealed that oxide-induced defect states promote the formation of self-trapped excitons, which enhance the interaction between charge carriers and molecular oxygen and the generation of superoxide radicals.[24] More recently, Li *et al.* reported that photo-induced redox reactions play a key role in the degradation of tin–lead perovskite solar cells. Illumination generates superoxide (O_2^-) that oxidizes Sn^{2+} to Sn^{4+}, triggering Pb^{2+} accumulation and irreversible phase changes. This process leads to lattice damage and performance loss, underscoring the importance of controlling redox chemistry for device stability.[25] To date, several strategies have been developed to suppress the redox activity of perovskites,[26] including stress release, and defect passivation.[27–29] One representative approach is the utilization of Eu^{3+}/Eu^{2+} redox pairs, which continuously oxidize Pb^0 and reduce I^0 defects in $FAPbI_3$-based PSCs, resulting in enhanced power conversion efficiency (PCE) and device durability.[30] Despite this progress,[31–34] several factors contribute to the redox reaction, and are interwoven

Key Laboratory for Ultrafine Materials of Ministry of Education, Shanghai Engineering Research Center of Hierarchical Nanomaterials, Shanghai Frontiers Science Center of Optogenetic Techniques for Cell Metabolism, School of Materials Science and Engineering, East China University of Science and Technology, Shanghai 200237, China. E-mail: syang@ecust.edu.cn, yhou@ecust.edu.cn
† Rui Yang and Xinyi Liu contributed equally to this work.

with each other under operational conditions. Therefore, it is essential to scrutinize the redox mechanisms under diverse operational conditions, which would help us improve the long-term stability of the solar cell devices.

In this study, we investigate the redox reaction mechanism occurring in PSCs fabricated on different substrates and under varying environments. We demonstrate that oxygen is the primary factor driving the oxidation degradation of PSCs, other than the spectral component of irradiation or transport layers. Specifically, in an oxygen-rich environment, perovskites undergo accelerated defect formation, including I_2 and I_3^- species, which severely compromise device performance. In contrast, under oxygen-deficient conditions, prolonged external stimuli lead to negligible degradation, highlighting the significant role of surface oxygen in driving the degradation process. Our findings underscore that oxygen is one of the key factors responsible for perovskite degradation in oxygen-containing conditions, shedding light on the design and assemble of stable PSCs.

Results and discussion

We spin-coated perovskite films onto various types of transport layers to analyze the impact of interfacial structure on the redox kinetics, including oxide layers (NiO_x, SnO_2, TiO_2), self-assembled layers: [2-(3,6-dimethoxy-9*H*-carbazol-9-yl)ethyl] phosphonic acid (MeO-2PACz), and organic layers: poly(3,4-ethylenedioxythiophene):poly(styrene sulfonate) (PEDOT:PSS) for characterization. Subsequently, the films were immersed in a toluene solution and exposed to four distinct conditions for 10 hours: (1) nitrogen environment (N_2), (2) nitrogen environment with light exposure (light-N_2), (3) oxygen environment (O_2), and (4) oxygen environment with light exposure (light-O_2). To establish a pure oxygen environment, high-purity O_2 gas was introduced into a custom-fabricated transparent chamber until complete atmospheric replacement was achieved. This sealed system enabled precise control of the gaseous environment during the treatment period. The perovskite composition investigated in this work is $Cs_{0.05}FA_{0.81}MA_{0.14}PbI_{2.85}Br_{0.15}$. Further details of the materials and experimental procedures are provided in the SI.

As shown in Fig. 1(a), the solution remained colorless under N_2, while a slight discoloration was observed under light-N_2. Notably, a visible magenta coloration developed under O_2, and this color change became significantly more intense under light-O_2. These results clearly demonstrate that perovskite films undergo substantial degradation in oxygen-rich environments, with light exposure further accelerating this process. This pronounced trend was consistently observed across different charge transport layers, highlighting oxygen as a critical factor in the redox reaction of perovskite solar cells.

The degradation mechanism should be related to the oxidation of I^- to I_2. Under oxygen-rich conditions, the perovskite film reacts with oxygen, leading to the oxidation of the I^- ions present in the perovskite structure. This process results in the formation of molecular I_2, which is responsible for the magenta color observed in the solution.[35] The light exposure further accelerates this oxidation process by increasing the rate of charge carrier generation, which facilitates the oxidation reaction.[23]

Ultraviolet-visible (UV-vis) spectra in Fig. 1(b) reveal a pronounced absorption peak at 500 nm for the magenta liquid, which corresponds to the characteristic signal of molecular I_2.[36] Fig. 1(c) illustrates the absorbance trends, and by integrating the data from Fig. 1, we can both qualitatively and quantitatively confirm that perovskite films degrade under oxygen-rich conditions, with light exposure further accelerating the degradation rate. Specifically, the I_2 content in perovskite films with various transport layers under light-O_2 is approximately ten times higher than that observed under light-N_2. However, under N_2, the films did not exhibit significant I_2 evolution after prolonged light exposure. Similarly, when the samples are under O_2, the I_2 content is eight times greater than when under N_2. These results demonstrate the fast degradation rate under oxygen-rich conditions.

We further investigated the redox processes of perovskite films on different substrates (PEDOT:PSS and NiO_x) under UV irradiation. 10-hour toluene immersion tests were conducted under four distinct atmospheric conditions: N_2, ultraviolet-irradiated nitrogen (UV-N_2), O_2, and ultraviolet-irradiated oxygen (UV-O_2). As illustrated in Fig. S1, a negligible color change was observed under N_2, while a light pink coloration appeared under UV-N_2. This is consistent with previous studies indicating that, even in an inert atmosphere, UV exposure can excite charge carriers in perovskite films, leading to defect formation, ion migration, and subsequent structural degradation.[37] Nevertheless, the discoloration under UV-N_2 was markedly less intense than that observed in oxygen-rich atmospheres. Fig. 1(d) quantitatively reveals that the I_2 concentration under UV-O_2 is approximately 3.1 times higher than that under UV-N_2, underscoring the synergistic impact of oxygen and UV light in accelerating film degradation.[38] Even when exposed to O_2, the I_2 content exceeded that under UV-N_2. Both qualitative and quantitative analyses consistently confirm that oxygen is the dominant factor driving perovskite degradation, irrespective of light exposure.

To investigate the synergistic effect of moisture and oxygen on perovskite degradation, we immersed films in a toluene solution containing 0.2% (v/v) water and exposed them for 10 hours under N_2, light-N_2, O_2, and light-O_2. In the presence of water, the degradation trends are consistent with those observed under anhydrous conditions (Fig. S3a and c), quantitative analysis (Fig. S3d) reveals that under light-O_2, the water present synergistically accelerates degradation, increasing the I_2 concentration by approximately 7.2% relative to the anhydrous environment. Under O_2, there is about a 2% increase in I_2 concentration. This conclusion is highly consistent with the findings of our study, further confirming that oxygen serves as the primary driver of perovskite lattice degradation, while water acts as a synergistic accelerator, facilitating the disruption of the crystal structure and organic components, thereby

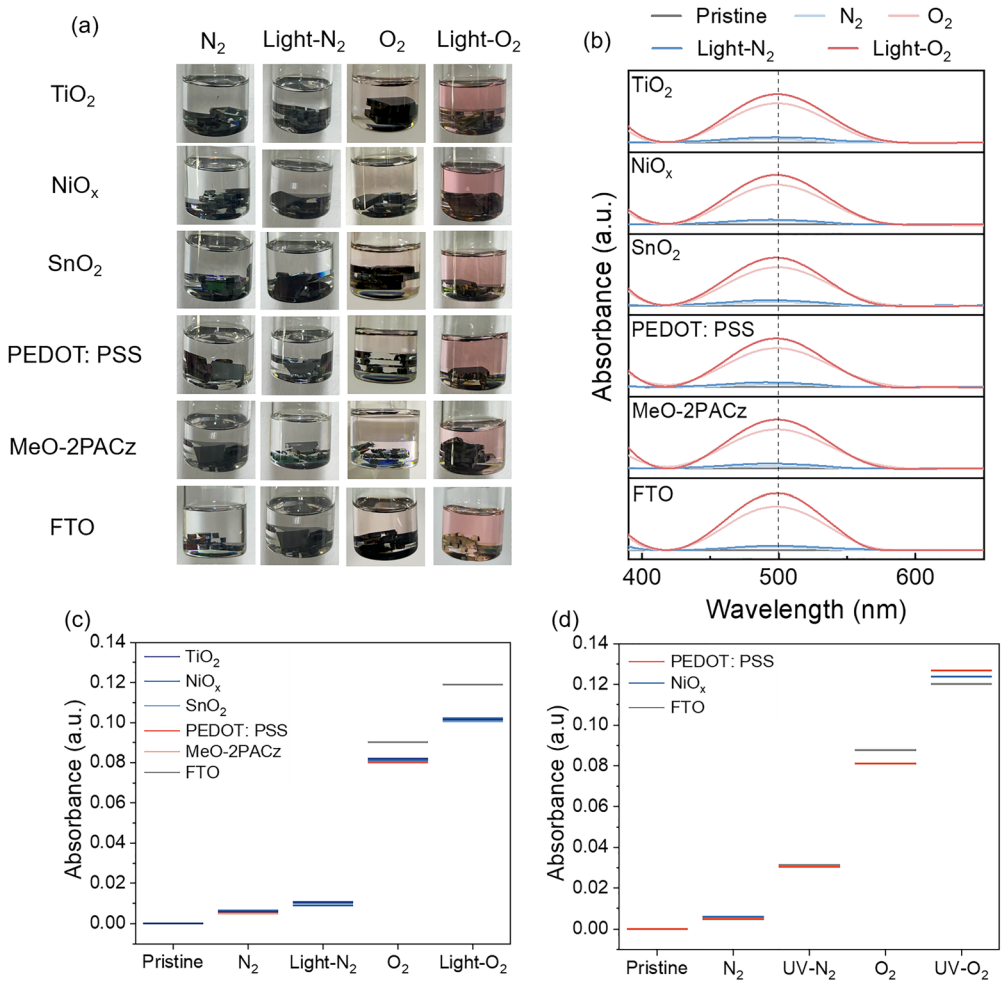

Fig. 1 (a) Perovskite films coated with different transport layers immersed in toluene under four distinct conditions for 10 hours: N_2, light-N_2, O_2 and light-O_2. A white LED of 100 mW cm^{-2} was used for the experiment. "FTO" refers to perovskite film coated on fluorine-doped tin oxide (FTO) without transport layers. (b) UV-vis spectra of the toluene extracts from perovskite films aged under four different environmental conditions. (c) Absorbance of I_2 signals determined by the UV-vis spectra of toluene solution, which has immersed the perovskite films for 10 hours under the four specified conditions. "Pristine" refers to freshly prepared perovskite films with various transport layers, directly immersed in toluene without any treatment. (d) Absorbance of I_2 signals of the toluene solutions, which were obtained by immersing perovskite film with different transport layers under certain conditions for 10 hours.

expediting the overall degradation of the material.[39] To further investigate this, we extended our study to pure $FAPbI_3$ and a Sn–Pb alloy perovskite ($Cs_{0.05}(FA_{0.7}MA_{0.5})_{0.95}Sn_{0.15}Pb_{0.85}I_3$) under identical conditions. Both compositions show degradation trends consistent with Cs/FA/MA perovskite but generate slightly more molecular I_2 under O_2 and light-O_2 (Fig. S4e). The accelerated degradation observed in $FAPbI_3$ is primarily attributed to residual PbI_2 resulting from its two-step fabrication process, which may act as reactive sites facilitating degradation.[40,41] In the Sn–Pb alloy, the enhanced degradation rate is likely due to the oxidation of Sn^{2+} ions, promoting the formation of reactive iodine species.[42] These findings confirm that the degradation mechanism proposed herein is consistent across representative perovskite systems, thereby reinforcing its broad applicability.

As shown in Fig. 2(a), Raman spectra of perovskite films exposed to oxygen-rich conditions exhibit a prominent peak at 169 cm^{-1}, which can be ascribed to the formation of molecular I_2.[23] Additionally, the Raman peaks at 114 cm^{-1} and 141 cm^{-1}, which are attributed to I_3^-,[35] exhibit significantly higher intensity compared to the peaks observed in films treated in an N_2 atmosphere. *In situ* Raman spectroscopy (Fig. S5) demonstrates that the combined application of stepwise heating and UV illumination under an O_2 atmosphere accelerates degradation and allows for the direct detection of molecular I_2, providing additional support for the proposed oxidation mechanism. This observation evidences that the major redox products are I_3^- and I_2 species in perovskite films under oxygen-rich conditions.

X-ray photoelectron spectroscopy (XPS) was conducted to investigate the evolution of the Pb 4f and I 3d peaks in the perovskite films under four different treatment conditions. As shown in Fig. 2(b), the pristine perovskite film exhibits the characteristic Pb^{2+} binding energy at 138.00 eV (Pb $4f_{7/2}$),[43] indicating a stable, undegraded state. Under light-N_2, the Pb 4f peak shifts slightly to ~138.15 eV, suggesting minimal

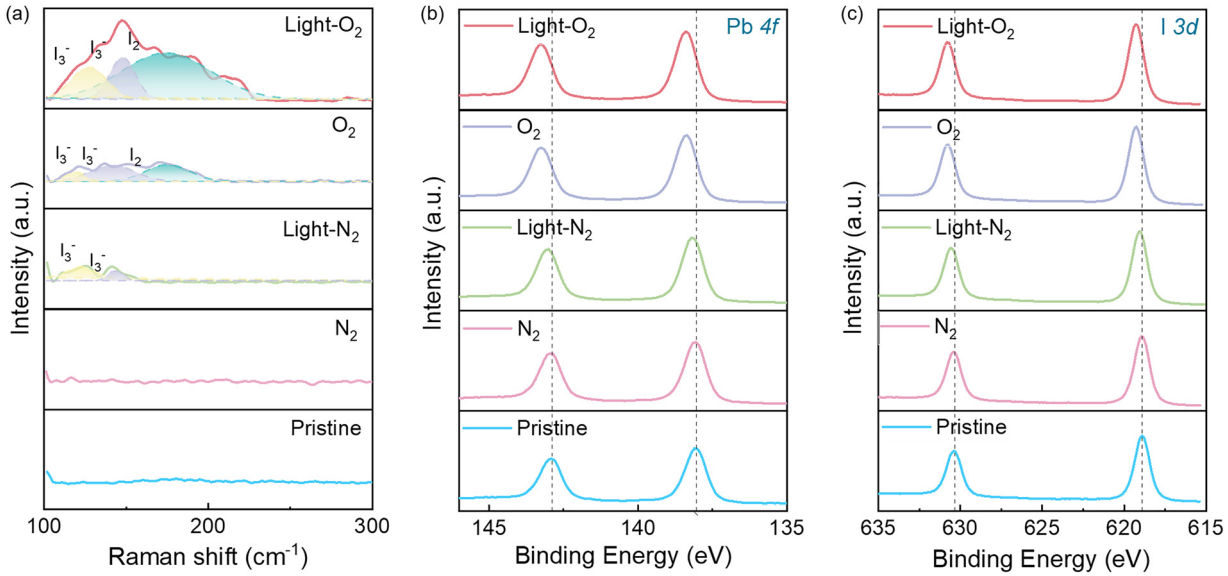

Fig. 2 (a) Raman spectra of perovskite subjected to different conditions for 10 hours. (b) Pb 4f XPS spectra subjected to different conditions for 10 hours. (c) I 3d XPS spectra subjected to different conditions for 10 hours.

chemical changes and weak degradation in the absence of oxygen. In contrast, under light-O_2 conditions, the Pb $4f_{7/2}$ peak further shifts to ~138.40 eV, likely associated with oxygen-induced degradation. The binding energy shift under light-O_2 is more obvious than that under light-N_2, demonstrating the synergistic effect of light and oxygen in accelerating the degradation of the perovskite film. The observed shift toward higher binding energy indicates a reduced electron density around Pb^{2+}, associated with lattice degradation and Pb–I bond instability, while the impact under inert conditions is negligible.[44] As shown in Fig. 2(c), the I 3d spectrum of the pristine perovskite film exhibits the characteristic binding energy of I^- at 619.00 eV (I $3d_{5/2}$),[45] indicating a chemically stable state. Under light-N_2, the peak shifts slightly to 619.09 eV, reflecting minor changes with minimal degradation. Under light-O_2 conditions, the I 3d peak shifts further to 619.25 eV, which is approximately 0.25 eV higher than the pristine state, indicating the larger chemical changes induced by the synergistic effect of light and oxygen. During this process, I^- undergoes electron loss *via* photo-induced oxidation in the presence of oxygen, thereby significantly accelerating the degradation of iodine species within the perovskite lattice.[46,47]

To evaluate the performance and stability of the devices under different conditions, we fabricated ITO/MeO-2PACz/perovskite/[6,6]-phenyl-C_{61}-butyric acid methyl ester ($PC_{61}BM$)/BCP/Ag solar cells. These devices were placed under the four predefined environmental conditions: N_2, light-N_2, O_2, and light-O_2, and their current density–voltage (*J*–*V*) characteristics were subsequently measured under AM 1.5G simulated sunlight. For the unencapsulated device, the PCE exhibited a slight improvement of 1.22% under N_2, while moderate degradation (1.47% loss) was observed under light-N_2, indicating minimal impact in the absence of oxygen. However, exposure to O_2 led to a significant efficiency drop of 6.69%, which was further aggravated under light-O_2, with the PCE declining by 18.91% (Fig. 3c). To mitigate oxygen-induced degradation, encapsulated devices were further evaluated under the same environmental conditions. As shown in Fig. 3(b) and (d), encapsulation effectively isolated the perovskite films from oxygen, resulting in negligible efficiency changes after 10 hours of exposure to all four environments. The operational stability of the devices was further evaluated by tracking the maximum power point (MPP). As shown in Fig. 3(e), under light-O_2, unencapsulated devices degraded rapidly to 50% of their initial efficiency within just 5 hours during MPP tracking, whereas encapsulated devices retained 99% and 98% of their initial efficiency under light-N_2 and light-O_2, respectively, even after 200 hours. The MPP tracking results clearly demonstrate that encapsulation is an effective strategy to mitigate oxygen-induced degradation.

XRD patterns in Fig. S6 reveal a significant acceleration of perovskite film degradation under O_2 and light-O_2 conditions, as evidenced by the intensified PbI_2 diffraction peak at ~11.8°.[48,49] SEM images of films aged for 10 hours under N_2 and light-N_2 (Fig. S4) show no significant morphological changes. Samples aged in O_2 (Fig. S5a) exhibited mild surface roughening and the appearance of PbI_2 nanoparticles. More pronounced degradation is observed under light-O_2 (Fig. S5b), featuring increased surface roughness, void formation, and more PbI_2 accumulation, consistent with the XRD data.[50] These morphological and structural observations further illustrate the compounding effect of oxygen and illumination, reinforcing their central role in triggering decomposition pathways. In particular, light exposure in oxidative environments facilitates the formation of reactive oxygen species (ROS),[51] which leads to a significant reduction in device performance.

A deeper investigation into the carrier dynamics and defect characteristics of the material under oxygen-rich conditions was conducted by performing steady-state photoluminescence

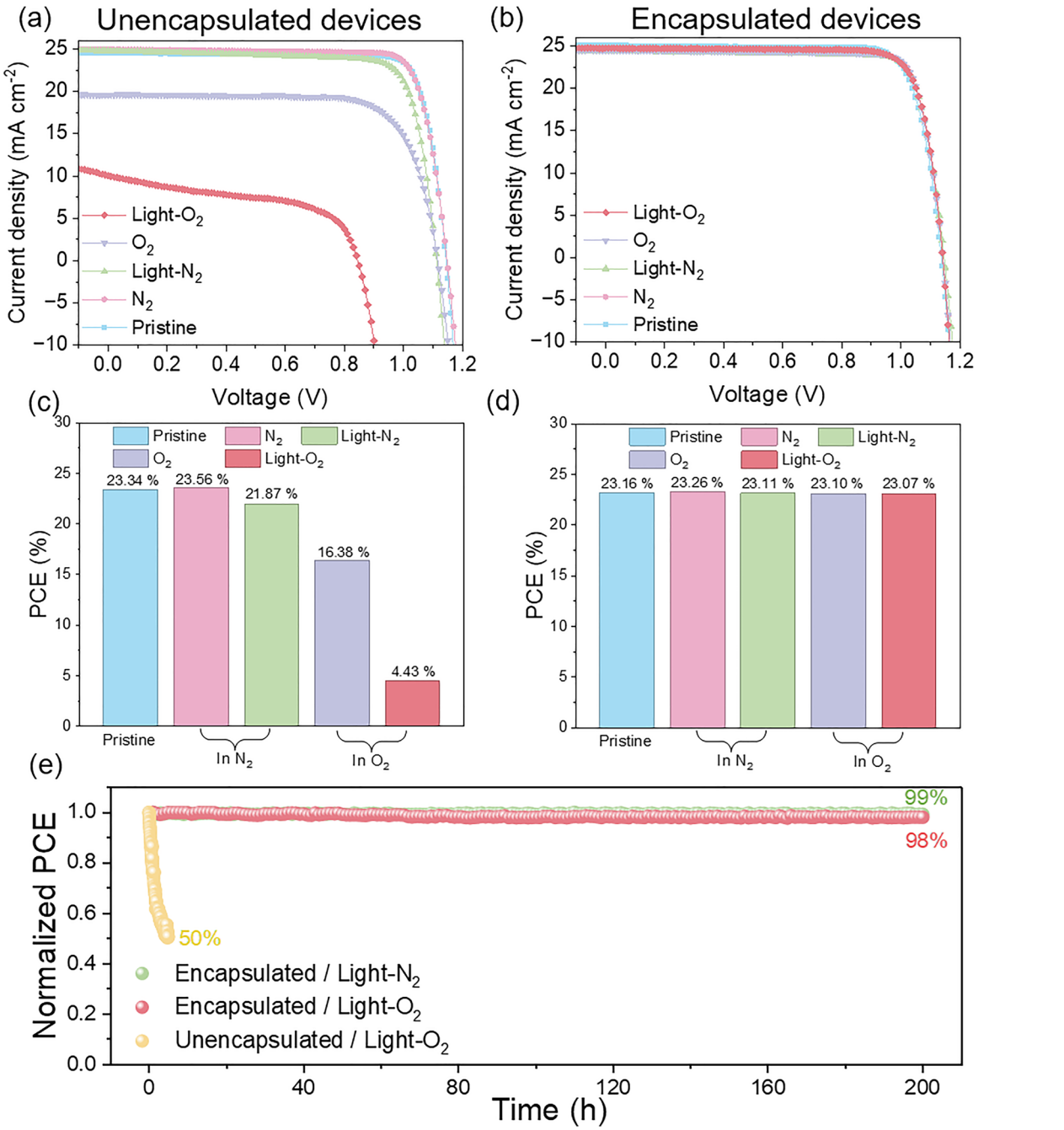

Fig. 3 (a) and (b) *J–V* characteristics of unencapsulated (a) and encapsulated (b) perovskite solar cells with the architecture ITO/MeO-2PACz/perovskite/PCBM/BCP/Ag, measured under AM 1.5G illumination. (c) and (d) PCE of unencapsulated devices (c) and encapsulated devices (d) under different environmental conditions. (e) Maximum power point (MPP) tracking of encapsulated and unencapsulated devices measured under continuous illumination conditions. Devices were tested under light-O_2 and light-N_2 atmospheres at 55 °C with an illumination intensity of 100 mW cm^{-2}.

(PL) and time-resolved photoluminescence (TRPL) measurements. The excitation light for both PL and TRPL measurements was incident from the air side. As depicted in Fig. 4(a), the perovskite films exposed to N_2 and light-N_2 atmospheres exhibited strong and sharp PL emission centered at approximately 790 nm,[52,53] indicating high radiative recombination efficiency and low defect density. Conversely, the samples exposed to O_2 environments, regardless of light exposure, exhibit a pronounced reduction in PL intensity along with a noticeable blue shift of the emission peak. This blue shift is indicative of an increase in bandgap energy, which can be attributed to oxygen-induced degradation of the perovskite lattice. It should be noted that I^- ions within the structure are susceptible to oxidation by O_2 molecules under photoexcitation, according to the reaction:

$$2I^- + \frac{1}{2}O_2 + H_2O \rightarrow I_2 + 2OH^-$$

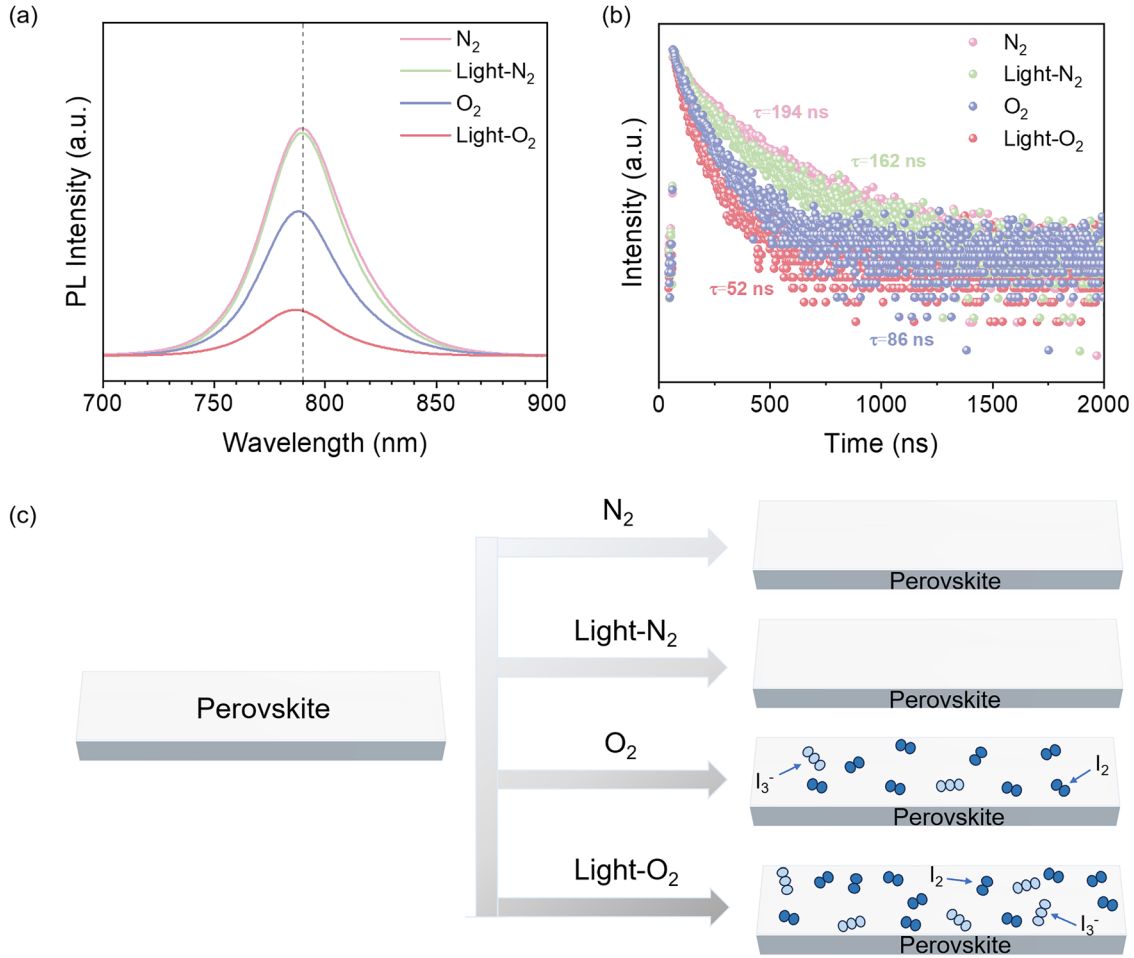

Fig. 4 (a) Steady-state and (b) time-resolved PL spectra of perovskite films under different conditions. The incident excitation light was irradiated from the air side. (c) Schematic illustrating the degradation behavior of perovskite films under different environmental conditions: N_2, light-N_2, O_2, and light-O_2.

The loss of I^- and the generation of I_2 disrupt the integrity of the $[PbI_6]^{4-}$ octahedral framework, resulting in defect formation, and the deterioration of the film's optoelectronic quality.[54] A substantial decline in PL intensity is observed upon O_2 exposure, reducing it to approximately two-thirds of that under N_2. This effect becomes markedly more severe when illumination is introduced, with the PL intensity decreasing nearly fivefold.

Fig. 4(b) displays the TRPL decay curves of perovskite films under different conditions. The perovskite films showed negligible changes in average carrier lifetime under N_2 and light-N_2 conditions, consistent with the degradation trends discussed earlier. Upon exposure to O_2, the carrier lifetime markedly decreases to ~86 ns, suggesting a substantial enhancement of nonradiative recombination pathways. This effect becomes even more severe under light-O_2 conditions, where the lifetime further shortens to ~52 ns, amounting to a reduction of nearly three-quarters compared to the N_2 baseline.[55–57] Overall, these results underscore the pivotal role of oxygen in accelerating perovskite degradation. Regardless of illumination, oxygen exposure leads to increased defect densities, reduced carrier lifetimes, and bandgap widening, all of which collectively deteriorate the material's optoelectronic performance.

Conclusions

In summary, we investigated the redox reactions occurring in PSCs with different perovskite compositions and interfaces by exposing the devices to four distinct environmental conditions: N_2, light-N_2, O_2 and light-O_2. However, we found that neither the transport layers, nor the spectral components of light significantly contribute to the redox reaction, once the oxygen is absent. We unequivocally identify that oxygen is the dominant factor driving oxidative degradation in PSCs. Under oxygen-rich conditions, halide perovskites undergo accelerated photolytic decomposition and ion migration, facilitating the formation of defect species such as molecular I_2, and I_3^- species. These defects markedly impair charge transport and increase non-radiative recombination pathways, thereby degrading device performance.

The results emphasize that the role of oxygen must be stringently regulated in redox-related studies, as it profoundly

influences interfacial reactivity and redox kinetics. For instance, during toluene soaking experiments, trace amounts of oxygen are often unavoidable and can significantly alter the chemical environment at the interface.

Furthermore, during device fabrication, oxygen molecules may be adsorbed onto material surfaces, thereby promoting undesired oxidation reactions. Such surface-adsorbed oxygen can act as an intrinsic driving force for redox processes, particularly under device operational conditions or even post-encapsulation, ultimately compromising the long-term operational stability of the system. This work provides critical mechanistic insights into the redox kinetics of perovskite materials and offers guidance for the rational design of PSCs with enhanced long-term stability.

Author contributions

S. Yang and Y. Hou directed the research. R. Yang and Y. Liu performed the experiments and data analyses. Y. Zhu provided assistance with the SEM characterization. Q. Li provided assistance with the Raman characterization. R. Y. and X. L. wrote the manuscript. All the authors participated in writing and editing the manuscript and contributed their efforts to the discussion.

Conflicts of interest

There are no conflicts to declare.

Data availability

The data for the plots presented in this paper and other findings of this study are available from the corresponding author upon reasonable request.

All data supporting the findings of this study are available in the Supplementary Information accompanying this manuscript. Supplementary Information: Detailed descriptions of materials, characterization methods, synthetic procedures for perovskites in different systems, and all relevant experimental details. It includes UV–Vis, Raman, XRD, surface SEM, cross-sectional SEM, and additional supporting figures and data. See DOI: **https://doi.org/10.1039/d5qm00466g**.

Acknowledgements

This work was financially supported by the National Natural Science Foundation of China (22379044), Shanghai Pilot Program for Basic Research (22TQ1400100-5), Shanghai Municipal Natural Science Foundation (25ZR1401081), the Fundamental Research Funds for the Central Universities (JKD01251505, JKVD1251041), the Postdoctoral Fellowship Program of CPSF (GZC20250071), Shanghai Engineering Research Center of Hierarchical Nanomaterials (18DZ2252400), and Shanghai Titan Natural Science Development Foundation and Shanghai Frontiers Science Center of Optogenetic Techniques for Cell Metabolism (Shanghai Municipal Education Commission).

References

1 Y. Shen, T. Zhang and G. Xu, *et al.*, Strain Regulation Retards Natural Operation Decay of Perovskite Solar Cells, *Nature*, 2024, **635**, 882–889.
2 K. Zhao, Q. Liu and L. Yao, *et al.*, Peri-Fused Polyaromatic Molecular Contacts for Perovskite Solar Cells, *Nature*, 2024, **632**, 301–306.
3 Y. Liu, L. Zheng and K. Zhang, *et al.*, Enhancing the crystallinity and stability of perovskite solar cells with 4-*tert*-butylpyridine induction for efficiency exceeding 24%, *J. Energy Chem.*, 2024, **93**, 1–7.
4 J. Li, J. Duan and C. Zhang, *et al.*, Facet-orientation-enhanced Thermal Transfer for Temperature-Insensitive and Stable P-i-n Perovskite Solar Cells, *eScience*, 2025, **5**, 100372.
5 H. Bi, J. Liu and L. Wang, *et al.*, Double Side Passivation of Phenylethyl Ammonium Iodide for All Perovskite Tandem Solar Cell with Efficiency of 26.8%, *EcoEnergy*, 2024, **2**, 369–380.
6 W. Li, E. Martínez-Ferrero and E. Palomares, Self-assembled Molecules as Selective Contacts for Efficient and Stable Perovskite Solar Cells, *Mater. Chem. Front.*, 2024, **8**, 681–699.
7 NREL, **https://www.nrel.gov/pv/interactive-cell-efficiency**.
8 B. Dong, M. Wei and Y. Li, *et al.*, Self-Assembled Bilayer for Perovskite Solar Cells with Improved Tolerance Against Thermal Stresses, *Nat. Energy*, 2025, **10**, 342–353.
9 N. Liu, M. Liu and J. Dai, *et al.*, Nucleation Engineering to Strengthen Interface Contacts in Single-Crystal Perovskite Photovoltaics, *Angew. Chem., Int. Ed.*, 2025, **64**, e202500947.
10 J. Zhou, T. Wen and J. Sun, *et al.*, Phase-Stable Wide-Bandgap Perovskites with 2D/3D Structure for All-Perovskite Tandem Solar Cells, *ACS Energy Lett.*, 2024, **9**, 1984–1992.
11 X. Sun, W. Shi and T. Liu, *et al.*, Vapor-Assisted Surface Reconstruction Enables Outdoor-Stable Perovskite Solar Modules, *Science*, 2025, **388**, 957–963.
12 X. Zhao, P. Zhang and T. Liu, Operationally Stable Perovskite Solar Modules Enabled by Vapor-Phase Fluoride Treatment, *Science*, 2024, **385**, 433–438.
13 S. Li, Y. Jiang and J. Xu, *et al.*, High-Efficiency and Thermally Stable $FACsPbI_3$ Perovskite Photovoltaics, *Nature*, 2024, **635**, 82–88.
14 D. B. Khadka, Y. Shirai and M. Yanagida, *et al.*, Defect Passivation in Methylammonium/Bromine Free Inverted Perovskite Solar Cells Using Charge-modulated Molecular Bonding, *Nat. Commun.*, 2024, **15**, 882.
15 S. Wang, S. Zhang and X. Shi, *et al.*, Self-Cleaning Spiro-OMeTAD via Multimetal Doping for Perovskite Photovoltaics, *Nat. Commun.*, 2025, **16**, 4167.
16 S. Baumann, G. E. Eperon and A. Virtuani, *et al.*, Stability and Reliability of Perovskite Containing Solar Cells and Modules: Degradation Mechanisms and Mitigation Strategies, *Energy Environ. Sci.*, 2024, **17**, 7566–7599.
17 S. Liu, Z. Sun and X. Lei, *et al.*, Stable Surface Contact with Tailored Alkylamine Pyridine Derivatives for High-Performance Inverted Perovskite Solar Cells, *Adv. Mater.*, 2024, **37**, 2415100.

18 M. H. Zhang and Y. Z. Qiang, *et al.*, Mechanism and Regulation of Tensile-Induced Degradation of Flexible Perovskite Solar Cells, *Energy Adv.*, 2024, **3**, 1431–1438.
19 Z. Liang, Y. Zhang and H. Xu, *et al.*, Homogenizing Out-of-plane Cation Composition in Perovskite Solar Cells, *Nature*, 2023, **624**, 557–563.
20 B. P. Kore, M. Jamshidi and J. M. Gardner, The Impact of Moisture on the Stability and Degradation of Perovskites in Solar Cells, *Mater. Adv.*, 2024, **5**, 2200–2217.
21 F. Fu, S. Pisoni and Q. Jeangros, *et al.*, I_2 Vapor-Induced Degradation of Formamidinium Lead Iodide-based Perovskite Solar Cells under Heat-Light Soaking Conditions, *Energy Environ. Sci.*, 2019, **12**, 3074–3088.
22 B. Purev-Ochir, X. Liu and Y. Fujita, *et al.*, Oxygen-Induced Reversible Degradation of Perovskite Solar Cells, *Sol. RRL*, 2023, **7**, 2300127.
23 S. G. Motti, D. Meggiolaro and A. J. Barker, *et al.*, Controlling Competing Photochemical Reactions Stabilizes Perovskite Solar Cells, *Nat. Photonics*, 2019, **13**, 532–539.
24 F. Ambrosio, E. Mosconi and A. A. Alasmari, *et al.*, Formation of Color Centers in Lead Iodide Perovskites: Self-Trapping and Defects in the Bulk and Surfaces, *Chem. Mater.*, 2020, **32**, 6916–6924.
25 W. Li, Z. Li and S. Zhou, *et al.*, Unveiling the Nexus Between Irradiation and Phase Reconstruction in Tin-Lead Perovskite Solar Cells, *Nat. Commun.*, 2025, **16**, 506.
26 Y. Zhu, X. Liu and X. Sui, *et al.*, Intermediate-Phase Homogenization Through Intermolecular Interactions Toward Reproducible Fabrication of Perovskite Solar Cells, *Adv. Energy Mater.*, 2025, 2500536.
27 Q. Li, Y. Zheng and H. Wang, *et al.*, Graphene-Polymer Reinforcement of Perovskite Lattices for Durable Solar Cells, *Science*, 2025, **387**, 1069–1077.
28 H. Wang, Q. Li and Y. Zhu, *et al.*, Photomechanically Accelerated Degradation of Perovskite Solar Cells, *Energy Environ. Sci.*, 2025, **18**, 2254–2263.
29 X. Leng, Y. Zheng and J. He, *et al.*, Mechanical Strengthening of a Perovskite-Substrate Heterointerface for Highly Stable Solar Cells, *Energy Environ. Sci.*, 2024, **17**, 4295–4303.
30 L. Wang, H. Zhou and J. Hu, *et al.*, A Eu^{3+}-Eu^{2+} Ion Redox Shuttle Imparts Operational Durability to Pb-I Perovskite Solar Cells, *Science*, 2019, **363**, 265–270.
31 R. Roy, M. M. Byranvand and M. R. Zohdi, *et al.*, All-Inorganic $CsPbI_2Br$ Perovskite Solar Cells with Thermal Stability at 250 °C and Moisture-Resilience via Polymeric Protection Layers, *Energy Environ. Sci.*, 2025, **18**, 1920–1928.
32 Y. Gao, Y. Gao and M. Wu, *et al.*, Enhancing the Stability of Perovskite Solar Cells and Modules by Two-Dimensional $(PM)_2PbI_2Cl_2$, *J. Mater. Chem. C*, 2025, **13**, 5332–5337.
33 H. Wang, S. Su and Y. Chen, *et al.*, Impurity-Healing Interface Engineering for Efficient Perovskite Submodules, *Nature*, 2024, **634**, 1091–1095.
34 G. Liu, G. Yang and W.-Q. Wu, *et al.*, Regulating Surface Metal Abundance via Lattice-Matched Coordination for Versatile and Environmentally-Viable Sn–Pb Alloying Perovskite Solar Cells, *Adv. Mater.*, 2024, **36**, 2405860.
35 N. Aristidou, C. Eames and I. Sanchez-Molina, *et al.*, Fast Oxygen Diffusion and Iodide Defects Mediate Oxygen-Induced Degradation of Perovskite Solar Cells, *Nat. Commun.*, 2017, **8**, 15218.
36 X. Lu, K. Sun and Y. Wang, *et al.*, Dynamic Reversible Oxidation-Reduction of Iodide Ions for Operationally Stable Perovskite Solar Cells under ISOS-L-3 Protocol, *Adv. Mater.*, 2024, **36**, 2400852.
37 W. Luo, H. Wen and Y. Guo, *et al.*, Simultaneous Ultraviolet Conversion and Defect Passivation Stabilize Efficient and Operational Durable Perovskite Solar Cells, *Adv. Funct. Mater.*, 2024, **34**, 2400474.
38 C. B. Fei, A. Kuvayskaya and X. Q. Shi, *et al.*, Strong-Bonding Hole-Transport Layers Reduce Ultraviolet Degradation of Perovskite Solar Cells, *Science*, 2024, **384**, 1126–1134.
39 J. Hidalgo, W. Kaiser and Y. An, *et al.*, Synergistic Role of Water and Oxygen Leads to Degradation in Formamidinium-Based Halide Perovskites, *J. Am. Chem. Soc.*, 2023, **45**, 24549–24557.
40 Y. Zhang, X. Wei and B. Yu, *et al.*, Residual PbI2 Conversion and Crystallization Control for Ambient-Air Fabrication of Industrially Viable Perovskite Solar Cells, *Adv. Funct. Mater.*, 2025, 2507346.
41 Y. Gao, H. Raza and Z. Zhang, *et al.*, R*eth*inking the Role of Excess/Residual Lead Iodide in Perovskite Solar Cells, *Adv. Funct. Mater.*, 2023, **33**, 2215171.
42 M. Yang, Y. Bai and Y. Meng, *et al.*, Sn-Pb Perovskite with Strong Light and Oxygen Stability for All-Perovskite Tandem Solar Cells, *Adv. Mater.*, 2025, **37**, 2415627.
43 M. De Keersmaecker, P. Dietrich and M. Bahri, *et al.*, Activated Corrosion and Recovery in Lead Mixed-Halide Perovskites Revealed by Dynamic Near-Ambient Pressure X-ray Photoelectron Spectroscopy, *J. Am. Chem. Soc.*, 2025, **10**, 8881–8892.
44 Y. Li, L. Dong and Y. Cai, *et al.*, Meticulous Design of High-Polarity Interface Material for $FACsPbI_3$ Perovskite Solar Cells with Efficiency of 26.47%, *Angew. Chem., Int. Ed.*, 2025, e202504902.
45 B. Du, Y. Lin and J. Ma, *et al.*, Buried Interface Management Toward High-Performance Perovskite Solar Cells, *Chem. Sci.*, 2025, **16**, 1876–1884.
46 Y. Liu, T. Ma and C. Wang, *et al.*, Synergistic Immobilization of Ions in Mixed Tin-Lead and All-Perovskite Tandem Solar Cells, *Nat. Commun.*, 2025, **16**, 3477.
47 Z. Peng, A. Vincze and F. Streller, *et al.*, Revealing Degradation Mechanisms in 3D/2D Perovskite Solar Cells under Photothermal Accelerated Ageing, *Energy Environ. Sci.*, 2024, **17**, 8313–8324.
48 Y. Bai, R. Tian and K. Sun, *et al.*, Decoupling Light- and Oxygen-Induced Degradation Mechanisms of Sn-Pb Perovskites in All Perovskite Tandem Solar Cells, *Energy Environ. Sci.*, 2024, **17**, 8557–8569.
49 J. Qian, J. He and Q. Zhang, *et al.*, Minimizing Interfacial Energy Losses in Inverted Perovskite Solar Cells by a Dipolar

Stereochemical 2D Perovskite Interface, *J. Energy Chem.*, 2024, **90**, 496–503.
50 Q. Zhuang, Z. Xu and H. Li, *et al.*, Molecular Polymerization Strategy for Stable Perovskite Solar Cells with Low Lead Leakage, *Sci. Adv.*, 2025, **19**, eado7318.
51 G. Grimaldi, I. Schuringa and J. J. Geuchies, *et al.*, Atmospheric Exposure Triggers Light-Induced Degradation in 2D Lead-Halide Perovskites, *ACS Energy Lett.*, 2024, **9**, 5771–5779.
52 X. Leng, Y. Zheng and J. He, *et al.*, Mechanical Strengthening of a Perovskite–Substrate Heterointerface for Highly Stable Solar Cells, *Energy Environ. Sci.*, 2024, **17**, 4295–4303.
53 J. Xie, Z. Zhou and H. Qiao, *et al.*, Modulating MAPbI3 Perovskite Solar Cells by Amide Molecules: Crystallographic Regulation and Surface Passivation, *J. Energy Chem.*, 2021, **56**, 179–185.
54 J. Chen, X. Wang and T. Wang, *et al.*, Determining the Bonding-Degradation Trade-Off at Heterointerfaces for Increased Efficiency and Stability of Perovskite Solar Cells, *Nat. Energy*, 2025, **10**, 181–190.
55 X. Wang, J. Li and R. Guo, *et al.*, Regulating Phase Homogeneity by Self-Assembled Molecules for Enhanced Efficiency and Stability of Inverted Perovskite Solar Cells, *Nat. Photonics*, 2024, **18**, 1269–1275.
56 Z. Xu, X. Sun and W. Hui, *et al.*, Optimizing Molecular Packing and Interfacial Contact via Halogenated N-Glycidyl Carbazole Small Molecules for Low Energy Loss and Highly Efficient Inverted Perovskite Solar Cells, *Angew. Chem., Int. Ed.*, 2025, e202503008.
57 X. Liu, H. G. Yang and S. Yang, *et al.*, Spontaneous Formation of Heterostructured Perovskite Films for Photovoltaic Application, *Chem. – Eur. J.*, 2023, **29**, e202202895.